Innovations in Renewable Energies Offshore – Guedes Soares & Wang (Eds)

Optimal geometry of a heaving point absorber considering an evolving Irish wave climate

N. Martinez-Iturricastillo, A. Ermakov & J.V. Ringwood
Centre for Ocean Energy Research Maynooth University, Maynooth, Co. Kildare, Ireland

A. Ulazia
Department of Energy Engineering University of the Basque Country, Eibar, Spain

ABSTRACT: An optimal geometry analysis of a heaving buoy point absorber Wave Energy Converter (WEC) is carried out, over its projected lifetime considering the evolution of seas states in a 31-year period (2025-2055). For this purpose, Commonwealth Scientific and Industrial Research Organisation (CSIRO) future wave data is employed on a grid point off the West of Ireland (10.5°W, 53°N). Yearly mean seas states defined by significant wave height H_s and peak wave period T_p are selected. Then, *Ansys AQWA* is used to estimate the power production of a traditional bottom-referenced point absorber, anchored to the ocean floor, operating under an energy maximising Simple and Effective controller. The evolution of yearly mean sea states together with the average power production for each geometry are presented. As well as an analysis of relative power decrease during the lifetime of the WEC, which shows that smaller WECs adapt best to the wave climate.

1 INTRODUCTION

Wave energy resource is still an untapped source of energy which has the potential to change the actual energy system by supplying an increasing electricity demand in a sustainable way. It has a higher availability compared to other renewable resources, higher energy density, and it is a predictable source of renewable energy. Unfortunately, wave energy is not in a commercial stage due to various challenges, one of them being the variability on the wave resource (wave-by-wave, hour-by-hour, site-by-site) (Guo and Ringwood 2021b).

Therefore, wave resource assessment is essential regarding Wave Energy Converters (WECs) design, which is conditioned by the site location. A study published by Arguilé-Pérez et al. (2022) analysed the most suitable WEC for different sites along the Galician coast based on metocean data.

Ireland has a high wave energy resource, it is the first landmass between the North Atlantic Ocean and Europe which endows the west coast of Ireland with strong swell and wind waves. In 2005 the Irish Marine Institute published a Wave Energy Resource Atlas, where the wave power was assessed along with its seasonality for two WEC devices. They concluded that the Irish west coast has higher wave energy density compared to the east coast, and that the annual accessible electrical energy was broadly equivalent to the one provided by a major supplier in Ireland (Marine Institute 2005).

A recent survey by Guo and Ringwood (2021a) on geometric optimization for WECs has underscored the importance of factoring in sea climate conditions during the geometry optimization process. This recognition stems from the understanding that such considerations can be both time-consuming and computationally intensive. Consequently, simplifications are frequently adopted, with the most prevalent sea state often serving as input data, while validation against extreme sea states is recommended to ensure device survivability.

Various studies have delved into different methods of geometry optimization. For example, Shadman et al. (2018) employed the Design of Experiments (DOE) approach to optimize the geometry of a heaving buoy point absorber. Similarly, Rava et al. (2022) conducted a geometry optimization for a point absorber, analyzing optimal Power Take Off (PTO) configurations alongside geometry variations, albeit without considering the climate effects on wave resources. Ulazia et al. (2020) incorporated long-term wave data spanning from 1979 to 2018 in their analysis of the optimal geometry of an Oscillating Water Column (OWC). Furthermore, Simonetti and Cappietti (2023) performed a geometry optimization for a floating OWC, utilizing future wave resource projections along the 20-meter bathymetric contour of the Atlantic Ocean and Mediterranean Sea.

In the interest of analyzing the performance of WECs under future wave climates, projections of wave resource are essential. Atmosphere-Ocean general Circulation Models are widely used to

DOI: 10.1201/9781003558859-4

characterize the climate system, but wind-wave resource are not parameterized as outputs of this models, therefore the wind-wave climate is limited to other climate variables such as precipitation and temperature.

The Coupled Model Intercomparison Project (CMIP) provides climate projections to better understand past, present and future climate changes, which are the foundations for the Intergovernmental Panel on Climate Change (IPCC) reports (Carvalho et al. 2022). Projections of global and regional wave climate systems under different future scenarios have been studied by various international research groups (Morim et al. 2018). Such as, CSIRO, who published global future projections for two climate scenarios (SSP126 and SSP585), WAVEWATCH III v6.07 (WW3) was employed to run the simulations in two CMIP6 Global Circulation Models (GCMs), EC-Earth3 and ACCESS-CM2 (Meucci et al. 2023). On the other hand, Jiang et al. (2023) run simulations using MASNUM-WAM for three future scenarios (SSP125, SSP245, SSP585) and wind forcing from FIO-ESM v2.0 from CMIP6.

In this paper, the authors conduct a geometry optimization of a heaving buoy wave energy converter while considering the influence of wave climate on the WEC's lifespan. The remainder of this paper is structured as follows: Section 2 elucidates the data utilized, while Section 3 describes the WEC model, simulation tools, performance function, and control strategy. Section 4 presents the main findings, and conclusions are drawn in Section 5.

2 WAVE CLIMATE DATA

In order to analyse the optimal geometry of a heaving buoy WEC during its lifetime projections of wave climate are required. Future projections of climate data are based on the Shared Socioeconomic Pathways (SSP) successive of the representative concentration pathways (O'Neill et al. 2017). Five scenarios have been defined: sustainable development (SSP1), middle-of-the-road development (SSP2), regional rivalry (SSP3), inequality(SSP4), and fossil-fueled development (SSP5) each of them having different approaches on different metrics such as, energy-system, urbanization, demographics, energy and land use, climate action, education and health (Riahi et al. 2017). Regarding greenhouse gas emissions in SSP1 CO2 emissions will be cut to net zero around 2070, while in SSP5 CO2 emissions will double by 2050 (Riahi et al. 2017).

The dataset used in this study is derived from the analysis performed by CSIRO. They run simulation in WW3 employing two CMIP6 global circulation models, EC-Earth3 and ACCESS-CM2, and forced them into two climate scenarios, SSP1 and SSP5, with two parametrizations for wind stress (CDFAC1.0, CDFAC1.08) (Meucci et al. 2023).

The dataset has a temporal resolution of 3 hours and a spatial resolution of 0.5°, it has global coverage and spans from 2015 until 2100. On this paper a single grid point is analysed off the West of Ireland (10.5° W, 53° N), and the time span analysed corresponds to the minimum for climate analysis and also encompasses the lifetime of a WEC, a total of 31 years from 2025 until 2055.

The results presented on this paper corresponds to the SSP5 scenario, the employed model is EC3-Earth, and the wind parametrization is CDFAC1.0.

2.1 *Data treatment*

The geometry analysis has been done in the yearly basis, therefore data has been arranged by years. A probability occurrence matrix for each year has been calculated employing 3-hourly data, as shown in Figure 1. To calculate the yearly average power of each geometry the mean sea state of each year has been selected. Significant wave height and peak wave period have been used to calculate the wave spectrum.

For the optimal geometry analysis of the WEC the mean value of each year is considered as the input for the model. Figure 2 illustrates the evolution of the yearly mean, median, and standard deviation of

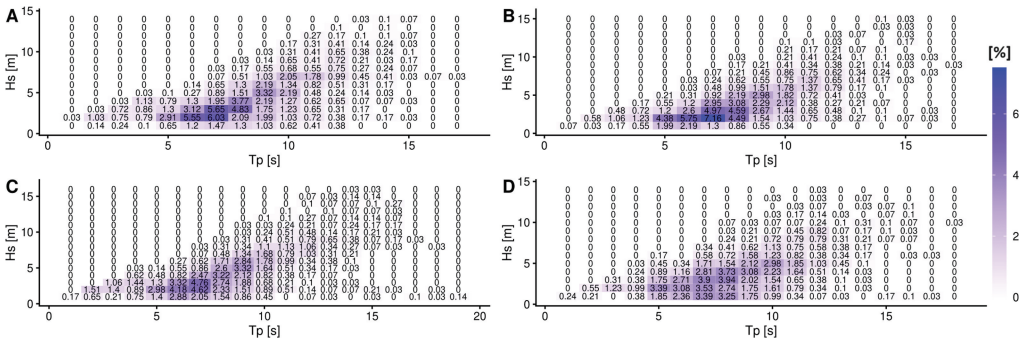

Figure 1. Probability occurrence matrix of sea states, significant wave height on the y axis and peak wave period on the x axis. A represents the probability occurrence matrix of the year 2025, B is 2035, C is 2045, and D is 2055.

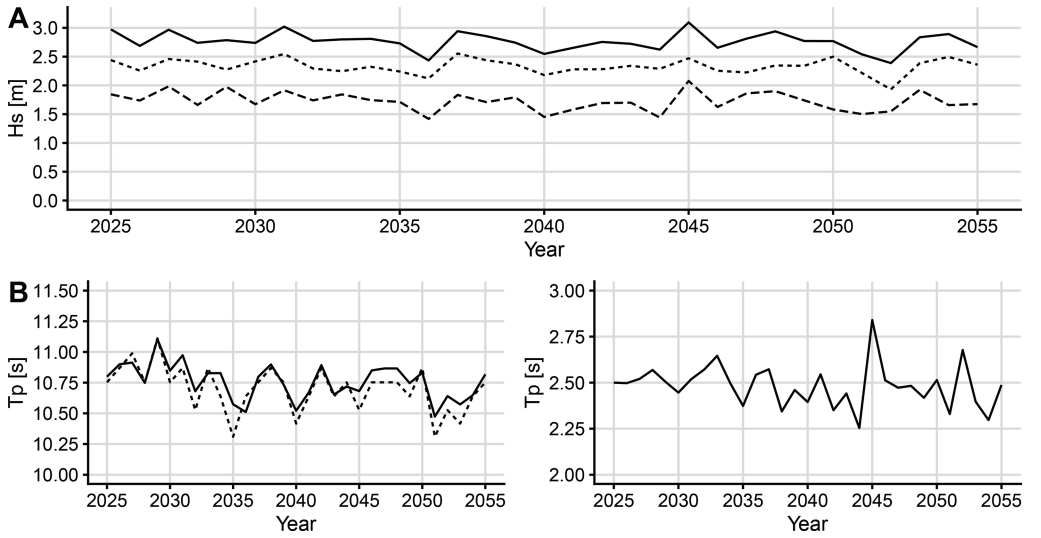

Figure 2. Evolution of mean, median and standard deviation of significant wave height and peak wave period in the West coast of Ireland (10.5°W, 53°N), from 2025 until 2055. A represents the significant wave height evolution, the solid black line is the mean, the dashed line in the middle is the median and the long-dashed line in the bottom represents the standard deviation. The two plots in B represent peak wave period evolution, on the left the solid black line is the mean and the dashed line is the median, the plot on the right is the standard deviation.

significant wave height and peak wave period over the analyzed time frame, which encompasses the lifespan of a WEC.

The employed dataset employed has been previously analysed for the whole available time period 2015-2100. A decrease in H_s, T_p and, consequently in wave power is expected in the analysed area during the 21st century (Ibarra-Berastegui et al.2023). Regarding the employed time span, the yearly mean H_s fluctuates from 2.4 to 3.1 meters and T_p from 10.5 to 11.1 seconds, this is shown in Figure 2.

3 METHODOLOGY

3.1 *Mathematical model for point absorber WEC*

Traditionally, the motion of the heaving buoy WEC in waves is described by Cummins' equation (Cummins, 1962). The current research focuses on a single degree-of-freedom problem, constraining movements to the vertical heave direction:

$$(m_h + m_\infty)\ddot{x}(t) + \int_0^t \dot{x}(\tau)k_r(t-\tau)d\tau + d_h\dot{x}(t) + k_s x(t) = f_{ex}(t) + f_{pto}(t), \quad (1)$$

where $x(t)$ denotes the vertical position of the buoy, m represents the mass of the buoy hull, and m_∞ indicates the added mass at infinite frequency. $k_r(t)$ stands for the impulse response function of radiation damping, k_s for hydrostatic stiffness, d_h for linearized viscous water damping, $f_{ex}(t)$ for wave excitation force, and $f_{pto}(t)$ for the force exerted by the power take-off (PTO) system.

The solution to Cummins' equation (1) for a body in waves can be acquired in the frequency domain using boundary element method (BEM)-based software (Ansys AQWA 2015). The resultant solutions for the heaving buoy hull displacement $X(\omega)$ at each specific frequency of a regular wave can be expressed in terms of the intrinsic system impedance, $Z_{hull}(\omega)$ (Falnes 2002), as:

$$X(\omega) = \frac{F_{ex}(\omega) + F_{pto}(\omega)}{j\omega Z_{hull}(\omega)}, \quad (2)$$

The intrinsic impedance of the system, referenced to the WEC hull, Z_{hull}, is given by:

$$Z_{hull}(\omega) = B(\omega) + j\omega\left[m_h + M_a(\omega) + m_\infty - \frac{k_s}{\omega^2}\right], \quad (3)$$

where $B(\omega)$ represents the radiation resistance, and $M_a(\omega)$ denotes the added mass after removing the singularity at infinite frequency m_∞.

3.2 *Performance function*

An estimate of the average power generation P_{avr} for a particular sea state can be obtained by integrating the product of the average power generation for a given wave frequency $P(\omega)$, and the probability distribution function for the wave frequencies of that sea state $p_{ss}(\omega)$ across all wave frequencies:

$$P_{avr} = \int_0^\infty P(\omega) p_{ss}(\omega) d\omega, \tag{4}$$

The probability distribution function for the wave frequencies $p_{ss}(\omega)$ can be derived from the Bretschneider wave spectrum distribution $p_{bs}(\omega)$, by normalizing it across all wave frequencies by its own integral:

$$p_{ss}(\omega) = p_{bs}(\omega) / \int_0^\infty p_{bs}(\omega) d\omega, \tag{5}$$

3.3 *Control strategy*

The study assumes that the PTO system is ocean bed-referenced and operates under a 'Simple and Effective' controller (Fusco and Ringwood 2013). In this control method, applied to the ocean bed-referenced WEC, the intrinsic impedance of the PTO system $Z^*_{pto}(\omega)$ is defined by the following equation:

$$Z^*_{pto}(\omega) = (2\alpha - 1) Re[Z_{hull}(\omega)] - j\, Im[Z_{hull}(\omega)], \tag{6}$$

where α represents a PTO damping tuning parameter, used to impose a constraints on the device displacement. However, when $\alpha = 1$, the traditional (unconstrained) complex conjugate control solution is obtained.

The corresponding response amplitude operators (RAOs) for displacement $X(\omega)$ and velocity $V(\omega)$, for the buoy hull, can be determined as follows:

$$X(\omega) = V(\omega)/(j\,\omega), \tag{7}$$

with

$$V(\omega) = \frac{F_{ex}(\omega)}{Z_{hull}(\omega) + Z^*_{pto}(\omega)} = \frac{F_{ex}(\omega)}{2\,\alpha\, Re[Z_{hull}(\omega)]}. \tag{8}$$

It is evident that an increase in the damping parameter α results in a decrease in both the magnitude and velocity of the buoy. The parameter α can be determined based on a maximum displacement constraint $|X| < X^{Max}$.

The maximum time averaged power production $P(\omega)$ in the frequency domain (Falnes 2002) due to the constrained displacement $|X(\omega)|$ can be evaluated as:

$$P(\omega) = \frac{1}{2} Re\left[Z^*_{pto}(\omega)\right] |V(\omega)|^2 = \frac{(2\alpha - 1)|F_{ex}(\omega)|^2}{8\,\alpha^2\, Re[Z_{hull}(\omega)]} \tag{9}$$

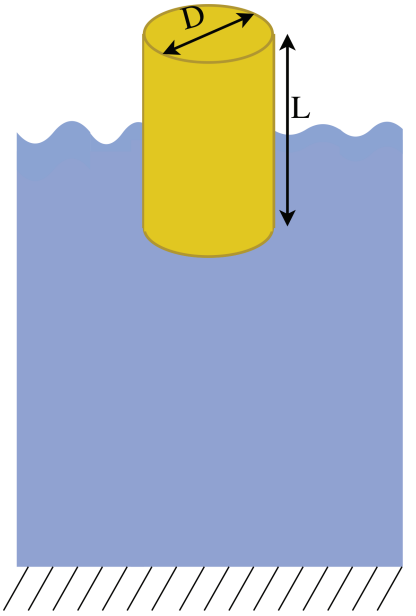

Figure 3. Semi-submerged heaving buoy WEC. D is the diameter of the cylinder, $R = D/2$ and L is the height.

3.4 *Optimization problem statement*

As stated in Section 2 the input of the model are yearly mean sea states which have been transformed into the frequency domain by employing the Bretschneider wave spectrum distribution $p_{bs}(\omega)$, Equation (5).

Sets of geometries and their average power have been calculated via Ansys AQWA, employing BEM (Ansys AQWA 2015). This analysis has been done considering two different scenarios in regards the radius (R) and height (L) of the semi-submerged cylindrical hull of the WEC. The Simple and Effective control strategy has been implemented, with the maximum displacement of the buoy hull limited to $X^{Max} = H_s/2$, where H_s represents the significant wave height. It is worth noting that the excitation force F_{ex} evaluated in Ansys AQWA is also directly proportional to the significant wave height H_s. In this study, a constant mass density of the device is assumed, with the mass centre located at the geometrical centre of the cylindrical hull. First, a scenario where $R = L$ is analysed, example shown in Table 1. In the second analysis, all the combinations of height and radius are considered, example in Table 2. In both cases the dimensions of the device are restricted from 1 to 6 meters in steps of 0.5 meters, giving a total of 11 possible dimensions for the first scenario where height and radius are the same and 121 geometries in the second scenario where all set of combinations are considered. Relative power generation decreases are calculated to asses the effect of wave climate on each geometry.

4 RESULTS

4.1 *Optimal geometry analysis*

A preliminary analysis has been carried out made where the radius and height of the heaving buoy cylinder are the same length, the average power generation per year is calculated for yearly mean sea state for a set of eleven geometries, encompassing radius values from 1 to 6 meters at 0.5 meters steps. In Figure 4 the average power production (y axis) is for the analysed time frame (2025-2055). Each coloured line represents a different geometry for a radius and height value of the device, it is shown that a bigger geometry will harness more energy compared to a smaller one. The annual average power depends on the wave climate, the effect of wave climate on the generated power is more pronounced on bigger geometries.

As the next step, a set of different heights is calculated for each radius, resulting in a total of 121 geometries. The cylinder radius and height range from 1 to 6 meters with a 0.5 meter increment, and all possible combinations are analyzed. In Figure 5, the effect of radius and height on the harnessed power is examined. The plots show the average power produced by a heaving buoy WEC in the year 2040, representing the mean sea state in that year. The power generated by a cylindrical heaving buoy can be increased by either increasing the cylinder's radius or decreasing its height.

In Figure 6, a depiction of the average power production is presented, spanning the investigative period from 2025 to 2055, corresponding to the operational lifespan of a WEC. This analysis focuses on cylinders with radii of both 3 meters (solid line) and 5 meters (dashed line), each varying in height according to specific device configurations, represented in colour lines. The observed power generation fluctuates annually in response to the prevailing mean sea state. As depicted in Figure 4, altering the radius of the cylinder induces corresponding shifts in power output, highlighting the sensitivity of the system to geometric variations.

4.2 *Climate adaptability*

Figure 6 clearly shows that there is no interaction with the geometries and the generated power, which means that the harnessed power varies based on the selected

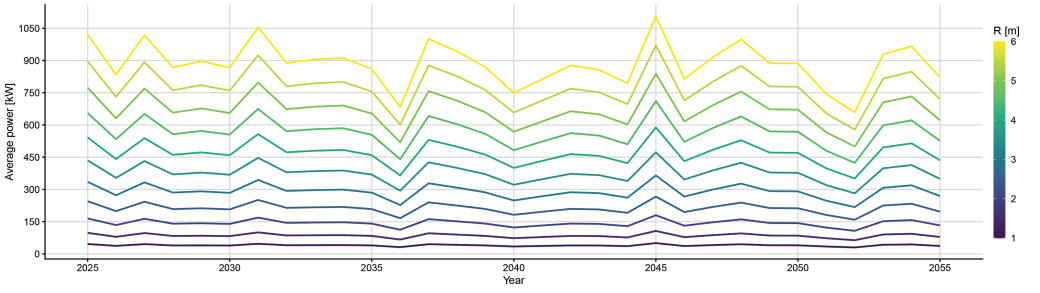

Figure 4. Yearly mean power production for different WEC geometry configurations in the West coast of Ireland (10.5°W, 53°N) from 2025 to 2055. Each line represents a geometry where $R = L$, results for eleven geometries are presented. The average wave power is in kilowatts and the radius is in meters.

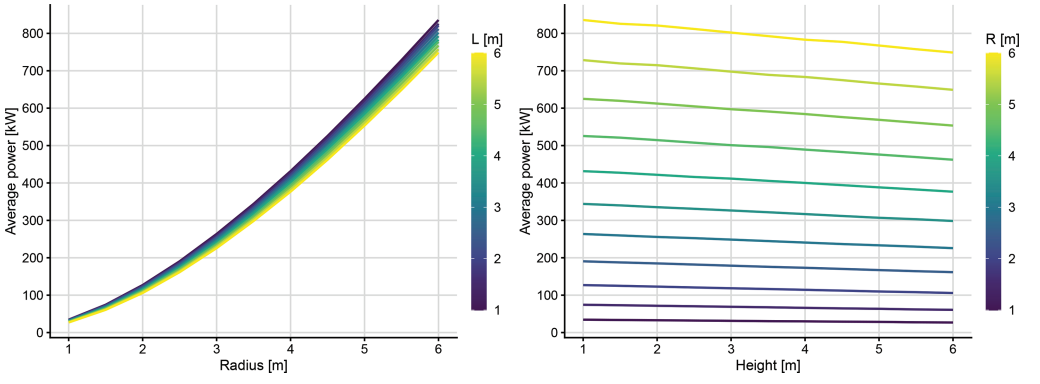

Figure 5. Mean power production for different WEC geometry configurations in the West coast of Ireland (10.5°W, 53°N) in 2040.

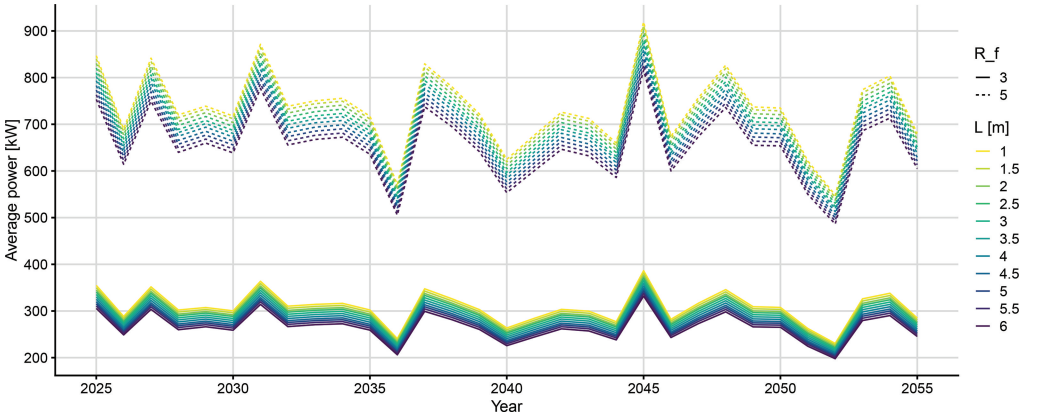

Figure 6. Average power production through the lifespan of a WEC for specific radii values, $R = 3$ meters (solid lines) and $R = 5$ meters (dashed lines), different cylinder heights are represented in colours.

Table 1. Average power production by a semi-submerged heaving buoy point absorber where $R = L$, for the yeas 2038-2042. Radius and height are in meters, while power is measured in kilowatts.

R = L	2038	2039	2040	2041	2042
1	21.5	18.4	13.9	16.2	18.6
1.5	45.7	39.3	29.6	34.5	39.6
2	77.1	66.2	49.8	58.1	66.8
2.5	114.6	98.2	73.7	86.2	99.2
3	157.0	134.4	100.7	117.9	136.0
3.5	203.8	174.3	130.4	152.8	176.5
4	254.1	217.1	162.1	190.2	220.1
4.5	307.4	262.3	195.6	229.7	266.2
5	363.1	309.5	230.5	271.0	314.4
5.5	420.9	358.4	266.5	313.7	364.4
6	480.1	408.4	303.4	357.4	415.7

geometry, but each geometry has an independent output. As shown in Figure 5 increasing the radius and decreasing the height of the WEC would lead to an increase in the harnessed energy. Therefore to maximize the generated power a device should have a big radius and small height, in fact, increasing the radius has a stronger effect compared to decreasing the cylinder's height.

To asses the capability of each geometry to adapt to the evolving wave climate, relative power generation decreases have been calculated for each geometry. Results are presented in Table 3. Greater radii and height have higher relative power losses. There are two geometries that perform best in terms of wave climate adaptability: $L = 1$; $R = 1.5$ and $L = 2$; $R = 1$. These two geometries are the most resistant geometries to the wave climate changes in terms of power production stability, since they have the lowest relative power generation reduction.

Table 2. Average generated power by different WEC geometry configurations on the year 2040, where 121 cases are considered. Radius (R) and height (L) are in meters, power is in kilowatts.

	L=1	L=1.5	L=2	L=2.5	L=3	L=3.5	L=4	L=4.5	L=5	L=5.5	L=6
R=1.0	34.4	33.7	33.0	32.1	31.4	30.5	30.0	29.1	28.6	27.4	27.0
R=1.5	74.3	73.1	71.6	70.3	68.9	67.6	66.1	64.7	63.5	61.8	60.8
R=2.0	126.9	125.0	122.9	120.6	118.4	116.5	114.3	112.2	109.8	108.0	105.7
R=2.5	190.5	187.6	184.9	181.9	178.9	175.8	173.2	170.2	167.1	164.1	161.5
R=3.0	263.6	259.7	255.7	252.5	248.6	244.6	240.7	236.7	233.3	229.8	225.7
R=3.5	344.0	340.1	335.3	331.0	326.5	321.7	316.8	311.8	306.9	303.0	298.3
R=4.0	431.6	427.4	421.8	416.1	411.6	405.7	400.1	394.2	388.2	382.6	376.7
R=4.5	525.6	521.2	514.6	507.8	501.0	496.3	489.2	482.7	476.0	469.3	462.2
R=5.0	624.9	619.6	612.4	604.9	597.2	591.2	584.3	576.2	568.9	561.2	553.5
R=5.5	728.5	719.6	714,925	706.5	697.7	689.2	683.4	675.0	665.9	657.9	649.1
R=6.0	835.8	825.7	821.1	811.8	802.1	792.7	783.1	777.4	767.6	757.7	748.8

Table 3 . Relative power generation decrease due to the predicted climate change for 2025-2055 years in percents. Results for the analysed set of geometries are presented. Radius (R) and height (L) are in meters.

	$L=1$	$L=1.5$	$L=2$	$L=2.5$	$L=3$	$L=3.5$	$L=4$	$L=4.5$	$L=5$	$L=5.5$	$L=6$
$R=1.0$	-6.38%	-6.17%	**-5.96%**	-5.97%	-5.97%	-5.98%	-6.15%	-6.25%	-6.23%	-6.21%	-6.19%
$R=1.5$	**-5.96%**	-5.97%	-5.97%	-5.98%	-6.16%	-6.25%	-6.23%	-6.21%	-6.20%	-6.20%	-6.16%
$R=2.0$	-5.97%	-5.98%	-6.26%	-6.24%	-6.23%	-6.21%	-6.20%	-6.20%	-6.16%	-6.17%	-6.13%
$R=2.5$	-6.24%	-6.23%	-6.22%	-6.20%	-6.21%	-6.18%	-6.16%	-6.16%	-6.13%	-6.11%	-6.10%
$R=3.0$	-6.20%	-6.21%	-6.19%	-6.16%	-6.15%	-6.14%	-6.12%	-6.11%	-6.09%	-6.08%	-6.09%
$R=3.5$	-6.16%	-6.17%	-6.13%	-6.12%	-6.11%	-6.10%	-6.13%	-6.09%	-6.09%	-6.11%	-6.17%
$R=4.0$	-6.11%	-6.11%	-6.1%	-6.13%	-6.08%	-6.09%	-6.10%	-6.14%	-6.20%	-6.26%	-6.31%
$R=4.5$	-6.09%	-6.09%	-6.09%	-6.11%	-6.15%	-6.18%	-6.24%	-6.28%	-6.33%	-6.39%	-6.44%
$R=5.0$	-6.16%	-6.18%	-6.22%	-6.26%	-6.30%	-6.33%	-6.37%	-6.42%	-6.46%	-6.32%	-6.33%
$R=5.5$	-6.31%	-6.35%	-6.37%	-6.40%	-6.45%	-6.49%	-6.34%	-6.32%	-6.60%	-6.64%	-6.69%
$R=6.0$	-6.46%	-6.41%	-6.32%	-6.32%	-6.54%	-6.62%	-6.66%	-6.68%	-6.73%	-6.75%	-6.66%

5 CONCLUSION

It has been shown that climate change affects the wave resource. The findings in this paper indicate that changes in wave resource directly influence the energy output of a heaving buoy WEC during its lifetime. While a cylindrical body with the largest radius and smallest height may optimize the power capture of a heaving buoy WEC, it is important to acknowledge that the generated power of the WEC will depend on the wave resource, and in this study is been shown that bigger cylindrical heaving buoys adapt worst to the wave climate changes.

This project has a set of inherited natural inaccuracy such as the use of linear hydrodynamics, the assumption of a constant mass for the device, or the selection of the mean sea state which is a limitation as seasonal effects are neglected, and it is known that waves are stronger during winter in Ireland. These assumptions could affect the predicted annual average power.

Future development on this project could analyse different WEC topologies as well as consider different geographical locations, and assess seasonality effects, or different metrics like the capture width ratio. Other aspects could be considered on the geometry selection such as, the survivability of the device under extreme weather conditions, or the effect on the Levelized Cost of Energy (LCoE), analysing the trade-off between the initial investment of producing the device and the harnessed energy during the WEC's lifespan. An assessment of the available ocean surface for the installation of the devices would also make a difference on the chosen geometry, whether different size of WECs can be installed together to increase the harnessed energy in arrays or if it is better to install bigger and lesser devices, but this analysis is out of scope in this paper.

ACKNOWLEDGEMENTS

This publication is part of a Grant from Science Foundation Ireland under Grant number 18/CRT/6049. This work was supported in part by a research grant from Science Foundation Ireland and the Sustainable Energy Authority of Ireland under SFI-IRC Pathway Programme 22/PATH-S/10793. This study is part of project PID2020-116153RB-I00 funded by Ministerio de Ciencia e Innovación/Agencia Estatal de Investigación MCIN/AEI/ 10.13039/501100011033.

REFERENCES

Ansys AQWA (2015). *Aqwa Theory Manual*. ANSYS, Inc.

Arguilé-Pérez, B., A. S. Ribeiro, X. Costoya, M. deCastro, P. Carracedo, J.M. Dias, L. Rusu, and M. Gómez-Gesteira (2022).Harnessing of different WECs to harvest wave energy along the galician coast(NWspain) *Journal of Marine Science and Engineering 10*(6),719. Number:6 Publisher: Multi disciplinary Digital Publishing Institute.

Carvalho, D., S. Rafael, A. Monteiro, V. Rodrigues, M. Lopes,and A. Rocha (2022). Howwell have cmip3, cmip5 and cmip6 future climate projection sport rayed the recently observed warming. *Scientific Reports 12* (1),11983.

Falnes,J.(2002).OceanWaves and Oscillating Systems: *Linear Interactions Including Wave-Energy Extraction. Cambridge University Press*.

Fusco, F. and J.V. Ringwood(2013).A simple and effective real-time controller for wave energy converters. *IEEE Transactions on Sustainable Energy* 4(1),21–30.

Guo,B. and J.V. Ringwood(2021a).Geometric optimisation of wave energy conversion devices: A survey. *Applied Energy 297*,117100.

Guo,B. and J.V.Ringwood(2021b).A review of wave energy technology from are search and commercial perspective. *IET Renewable Power Generation 15* (14),3065–3090.

Ibarra-Berastegui,G., J. Sáenz, A. Ulazia, A. Sáenz-Aguirre, and G. Esnaola (2023).Cmip6 projections for global offshore wind and wave energy production (2015–2100).*Scientific Reports 13*(1),18046.

Jiang, X., B. Xie, Y. Bao, and Z. Song (2023).Global3-hourly wind-wave and swell data for wave climate and wave energy resource research from 1950 to 2100. *Scientific Data 10*(1), 225. Publisher: Nature Publishing Group.

Marine Institute (2005). Accessible wave energy resource atlas 2005.Available: https://data.gov.ie/dataset/accessible-wave-energy-resource-atlas-2005/resource/8529c655-9afa-4a2a-8fc6-dbeef3f271cf [Accessed:19-April-2024].

Meucci, A., I. R. Young, M. Hemer, C.Trenham, and I.G. Watterson (2023).140 years of global ocean wind-wave climate derived from cmip6 access-cm2 and ec-earth3gcms:Global trends, regional changes, and future projections. *Journal of Climate* 36(6),1605–1631.

Morim, J., M.Hemer, N.Cartwright, D.Strauss, and F. Andutta (2018).On the concordance of 21st century wind-wave climate projections. *Global and planetary change 167*, 160–171.

O'Neill, B.C.,E. Kriegler, K.L. Ebi, E. Kemp-Benedict, K. Riahi, D.S. Rothman, B. J. VanRuijven, D. P. VanVuuren, J. Birkmann, K. Kok, et al. (2017).The roads ahead: Narratives for shared socioeconomic pathways describing world futures in the 21st century. *Global environmental change* 42,169–180.

Rava, M., P. Dafnakis,, V. Martini, G. Giorgi,, V. Orlando, G. Mattiazzo, G. Bracco, and A. Gulisano (2022).Low-cost heaving single-buoy wave-energy point absorber optimization for sardinia westcoast. *Journal of Marine Science and Engineering 10*(3), 397.

Riahi, K., D. P. Van Vuuren, E. Kriegler, J. Edmonds, B. C. O'neill, S. Fujimori, N. Bauer, K. Calvin, R. Dellink, O. Fricko, et al. (2017). The shared socioeconomic pathways and their energy, land use, and greenhouse gas emissions implications: An overview. *Global environmental change* 42,153–168.

Shadman, M., S. F. Estefen, C. A. Rodriguez, and I. C. M. Nogueira (2018). A geometrical optimization method applied to a heaving point absorber wave energy converter. *Renewable Energy 115*, 533–546.

Simonetti, I. and L. Cappietti (2023). Effects of projected wave climate changes on the sizing and performance of owcs: A focus on the mediterranean and atlantic european coastal waters. In *Proceedings of the European Wave and Tidal Energy Conference*, Volume 15.

Ulazia, A., G. Esnaola, P. Serras, and M. Penalba (2020). On the impact of long-term wave trends on the geometry optimisation of oscillating water column wave energy converters. *Energy 206*, 118146.